Translational Oncology
www.transonc.com

Volume 4 Number 3 June 2011 pp. 178–188 178

STAT3 Knockdown in B16 Melanoma by siRNA Lipopolyplexes Induces Bystander Immune Response *In Vitro* and *In Vivo*[1]

Aws Alshamsan*,†, Samar Hamdy†, Azita Haddadi‡, John Samuel†,2, Ayman O. S. El-Kadi†, Hasan Uludağ†,§,¶ and Afsaneh Lavasanifar†,§

*Department of Pharmaceutics, College of Pharmacy, King Saud University, Riyadh, Saudi Arabia; †Faculty of Pharmacy and Pharmaceutical Sciences, University of Alberta, Edmonton, Alberta, Canada; ‡College of Pharmacy and Nutrition, University of Saskatchewan, Saskatchewan, Canada; §Department of Chemical and Material Engineering, Faculty of Engineering, University of Alberta, Edmonton, Alberta, Canada; ¶Department of Biomedical Engineering, Faculty of Medicine and Dentistry, University of Alberta, Edmonton, Alberta, Canada

Abstract

Persistent activation of STAT3 plays a major role in cancer progression and immune escape. Therefore, targeting STAT3 in tumors is essential to enhance/reactivate antitumor immune response. In our previous studies, we demonstrated the efficacy of stearic acid–modified polyethylenimine (PEI-StA) in promoting small interfering RNA (siRNA) silencing of STAT3 in B16.F10 melanoma *in vitro* and *in vivo*. In the current study, we examine the immunologic impact of this intervention. Toward this goal, the infiltration and activation of lymphocytes and dendritic cells (DCs) in the tumor mass were assessed using flow cytometry. Moreover, the levels of IFN-γ, IL-12, and TNF-α in homogenized tumor supernatants were determined. Moreover, mixed lymphocytes reaction using splenocytes of tumor-bearing mice was used to assess DC functionality on siRNA/lipopolyplexes intervention. Our results demonstrated up to an approximately fivefold induction in the infiltration of $CD3^+$ cells in tumor mass on STAT3 knockdown with high levels of $CD4^+$, $CD8^+$, and NKT cells. Consistently, DC infiltration in tumor milieu increased up to approximately fourfold. Those DCs were activated, in an otherwise suppressive microenvironment, as evidenced by a high expression of costimulatory molecules CD86 and CD40. ELISA analysis revealed a significant increase in IFN-γ, IL-12, and TNF-α. Moreover, mixed lymphocytes reaction demonstrated alloreactivity of these DCs as assessed by high T-cell proliferation and IL-2 production. Our results suggest a bystander immune response after local STAT3 silencing by siRNA. This strategy could be beneficial as an adjuvant therapy along with current cancer vaccine formulations.

Translational Oncology (2011) 4, 178–188

Introduction

Immune evasion is a hallmark of cancer progression and development [1,2]. To evade immune detection and eradication, tumors possess a major strategy through persistent activation of signal transducer and activator of transcription 3 (STAT3) [3–6]. This downstream protein is a transcription factor that becomes activated in response to cytokines and growth factor receptor stimulation. On stimulation, STAT3 monomers get phosphorylated and then form homodimers or heterodimers that translocate to the nucleus to upregulate the expression of target genes. In a variety of tumor cells, activated STAT3 promotes transcription of genes responsible for cell survival and pro-

Address all correspondence to: Associate Prof Afsaneh Lavasanifar, PhD, # 4119 Dent/Pharm Centre, University of Alberta, Edmonton, Alberta, Canada T6G 2N8. E-mail: alavasanifar@pharmacy.ualberta.ca; or Dr. Aws Alshamsan, P.O. Box 2457, Riyadh 11451, Saudi Arabia. E-mail: aalshamsan@ksu.edu.sa

[1]This project was funded by operating grants to J.S. and A.L. (MOP 42407) and to H.U. (MOP 74452) from the Canadian Institute of Health Research.
[2]This article is dedicated to the memory of Dr John Samuel, a mentor and a friend, who initiated a research program encompassing this study.
Received 13 January 2011; Revised 24 March 2011; Accepted 24 March 2011

1944-7124/11
DOI 10.1593/tlo.11100

liferation, angiogenesis, metastasis, as well as immune escape [7,8]. For immune escape property, STAT3 impact appears at two levels: the cell-intrinsic level and the cell-extrinsic level. The cell-intrinsic mechanisms encompass changes in cancer cells that have resulted from persistently active STAT3. For instance, constitutively active STAT3 suppresses the production of the chemokines RANTES and IP-10 that are responsible for T-cell recruitment [3]. Another example is the down-regulation of the tumor cell surface expression of Fas receptor (CD95), which is a proapoptotic receptor involved in cytotoxic T lymphocyte (CTL)–dependent cytotoxicity [9]. Conversely, the cell-extrinsic level is orchestrated by the ability of STAT3 to mediate a cross-talk between cancer and immune cells [10–12]. In this scenario, tumor-derived factors (TDFs) produced by STAT3-active tumors induce the activation of STAT3 in multiple subsets of innate and adaptive immune cells [11,13]. On STAT3 hyperactivity, innate immune cells such as natural killer (NK) cells, tumor-associated macrophages, NKT cells, and neutrophils lose their ability of tumor inhibition or effective production of immunostimulatory molecules [11]. One of the most important affected cell subsets in this equation is dendritic cells (DCs), as they form the link between the innate and adaptive arms of the immune response owing to their ability as the most potent antigen-presenting cells. The immunosuppressive milieu induces the production of immunosuppressive TDFs that further inhibit DC maturation and results in the inhibition of T_H1-type immune response and CTL cytotoxicity [3]. Thus, in the presence of cancer, DC malfunction causes an immunologic paralysis leading to the potentiation of cancer progression [5,14]. Therefore, breaking this cycle of tolerance by targeting persistently active STAT3 in tumors is essential to reactivate the immune system for a robust antitumor response in an otherwise immunosuppressive microenvironment.

RNA interference mediated by small interfering RNA (siRNA) provides a very specific and effective modality to downregulate protein expression at the mRNA level [15]. Despite great potential, siRNA technology suffers from fundamental drawbacks such as low biologic stability, poor cell permeability, and unfavorable pharmacokinetic and biodistribution profile that hinder its progress from bench to bedside [16]. Therefore, it is essential to develop a delivery system that optimally delivers siRNA to its site of action while retaining its silencing activity [17].

We have recently developed a polymeric systems for siRNA delivery to B16 melanoma cells based on stearic acid (StA) substitution on polyethylenimine (PEI) backbone, where such modification led to better siRNA stability in biologic milieu, effective down-regulation of STAT3 at low siRNA doses, resulting in the inhibition of B16 cell growth both *in vitro* and *in vivo* [18]. Moreover, a reduction in the level of vascular endothelial growth factor (VEGF), an increase in interleukin-6 (IL-6) production, and a rise in caspase 3 activity in isolated tumor mass on siRNA intervention was noted [18]. In the present study, the effect of STAT3 down-regulation by its siRNA/stearic acid–modified polyethylenimine (PEI-StA) complexes in tumor cells on the trafficking and activity of tumor-derived immune cells including DCs has been investigated to assess whether effective knockdown of STAT3 in the effector phase can break the vicious cycle of immunosuppression in tumor microenvironment and lead to better antitumor immune responses.

Materials and Methods

Animals

All animal studies were conducted in accordance with the Canadian Council on Animal Care Guidelines and Policies with approval from the Animal Care and Use Committee: (Biosciences, Health Sciences or Livestock) for the University of Alberta. All experiments were performed using 4- to 6-week-old male mice. Male BALB/c and C57BL/6 mice were purchased from Jackson Laboratory (Bar Harbor, ME).

Materials

Branched PEI (25 kDa), triethylamine (TEA), 3-(4,5-dimethylthiazol-2-yl)-2,5-diphenyltetrazolium bromide (MTT), dimethyl sulfoxide, and stearoyl chloride (98.5%) were obtained from Sigma-Aldrich (St Louis, MO). Anhydrous ethyl ether and dichloromethane were purchased from Fisher Scientific (Fairlawn, NJ). Fetal bovine serum (FBS) was obtained from HyClone (Logan, UT). Dulbecco modified Eagle, RPMI-1640, L-glutamine, and gentamicin were purchased from Gibco-BRL (Burlington, Ontario, Canada). Mouse interleukin 2 (IL-2), IL-12, tumor necrosis factor α (TNF-α), and interferon-γ (IFN-γ) ELISA kit was purchased from e-Biosciences (San Diego, CA). Sequence-specific siRNA targeting murine STAT3 mRNA was purchased from Ambion (Austin, TX) (sense: 5′-GGACGACUUUGAUUUCAACtt-3′, antisense: 5′-GUUGAAAUCAAAGUCGUCCtg-3′). The nontargeting (NT) siRNA Silencer Negative Control no. 1 siRNA (catalog no. AM4635) and Silencer FAM-labeled Negative Control no. 1 siRNA (catalog no. AM4620), both purchased from Applied Biosystems (Foster City, CA). Caspase 3 assay kit, Nonidet P-40, protease inhibitor cocktails, and 4-nitrophenyl phosphate were purchased from Sigma-Aldrich. Antiphosphotyrosine (Y^{705}) STAT3 monoclonal antibody, anti-STAT3 antibody, and antiactin antibody (I-19) were purchased from Santa Cruz Biotechnology (Santa Cruz, CA). ECL Plus Detection Kit was purchased from GE Healthcare Life Sciences (Piscataway, NJ). Antimouse CD3 (FITC-labeled), CD4 (phycoerythrin [PE]-Cy5–labeled), CD8 (PE-Cy5–labeled), NK1.1 (PE-labeled), CD11c (FITC-labeled), CD86 (PE-labeled), and CD40 (PE-Cy5–labeled) mAbs, or corresponding isotype controls, were purchased from BD Biosciences (Mississauga, Ontario, Canada). EasySep Negative Selection Kit for T-cell isolation was purchased from Stem Cell Technologies (Vancouver, British Columbia, Canada).

Preparation of siRNA Complexes

PEI-StA was prepared by *N*-acylation of PEI with stearoyl chloride and characterized as described in Alshamsan et al. [19]. Then, in sterile Eppendorf tubes, equal amounts (μg) of siRNA and PEI or PEI-StA in PBS were incubated for 30 minutes at 37°C as previously described [18]. Samples were freshly prepared before each administration.

Assessing the Effect of Medium from Untreated and siRNA-Treated B16 Cells on In Vitro *DC Maturation and Function*

B16.F10 treatment. For STAT3 targeting, 1×10^5 B16 melanoma cells were incubated (in 24-well plates) for 36 hours at 37°C with titrated doses of anti-STAT3 siRNA (6.25-400 nM) delivered by PEI or PEI-StA complexes. Identical complexes of NT siRNA as well as untreated B16 cells were used as controls. To remove the uninternalized complexes, B16 medium was replenished after 8 hours of incubation. Then, cells were lysed, and levels of active phosphorylated STAT3 (p-STAT3) as well as total STAT3 were detected by Western blot (see below). The optical intensity of p-STAT3 band was quantified and normalized to actin protein band using ImageJ software (W. Rasband [2005], National Institutes of Health, Bethesda, MD; http://rsb.info.nih.gov/ij). The percentage of p-STAT3 silencing was

calculated at each dose by comparing the level of STAT3 in the test group *versus* the level of STAT3 in the untreated cells (considered as 100%). Simultaneously, on 96-well plate, cancer cell viability was determined by MTT assay and caspase 3 activity assay after the 36 hours of incubation with siRNA complexes; in these assays, a single concentration of siRNA was used (50 nM).

DC treatment. Primary DC culture was generated from bone marrow precursor of C57BL/6 mice femurs and propagated in complete RPMI-1640 in the presence of GM-CSF as previously described [20]. The purity of the DC population on day 7 was found to be between 70% and 75% based on the expression of CD11c on the semiadherent and nonadherent cell populations. To increase DC purity, semiadherent and nonadherent cells were isolated from primary culture on day 6 by thorough suspension in growth medium. Cells were centrifuged and resuspended in fresh complete RPMI-1640 in the presence of granulocyte-macrophage colony-stimulating factor and then transferred to new cell culture plates 24 hours before any manipulation. After this process, 95% of cells were confirmed to be positive for CD11c. Malfunctioned DCs at day 7 were generated by exposure to tumor-conditioned medium from B16.F10 melanoma culture (B16-CM) for 24 hours as previously described in Alshamsan et al. [21]. In brief, murine B16.F10 cells were grown and propagated in Dulbecco modified Eagle medium supplemented with 10% FBS at 37°C and 5% CO_2. After confluence, B16 cells were incubated with serum-free medium for 24 hours. This medium was collected and grouped according to the designated treatment into anti-STAT3 siRNA complexes treated (B16-CM/PEI and B16-CM/PEI-StA), NT siRNA complexes treated (B16-CM/PEI[NT] and B16-CM/PEI-StA[NT]), and untreated B16-CM. Thereafter, the conditioned medium from each treatment group was added to a primary DC culture, reaching a final B16-CM concentration of 50%. FBS was then supplemented to 10% final concentration in culture. After that, DC phenotypic maturation was evaluated by surface expression of CD40 and CD86 as analyzed by flow cytometry (FCM). Moreover, mixed lymphocytes reaction (MLR) was performed as described below to assess DC function as indicated by their capability to stimulate allogenic T-cell proliferation.

Western blot. Cells were collected and washed twice with ice-cold PBS. Then, sample tubes were imbedded in ice, and cells were lysed in lysis buffer containing 30 mM HEPES (pH 7.5), 2 mM Na_3VO_4, 25 mM NaF, 2 mM EGTA, 2% Nonidet P40, 1:100 protease inhibitor cocktails, 0.5 mM dithiothreitol, and 6.4 mg/ml phosphatase substrate 4-nitrophenyl phosphate. Cell lysates were centrifuged for 20 seconds at 16,000*g*. Thereafter, NaCl was added to samples to final concentration of 420 mM, cell lysates were centrifuged for 20 minutes at 16,000*g*, the supernatant was transferred to new tubes, and pellets were discarded. Total protein extract was determined by Micro BCA Protein Assay Kit. Equal amounts of protein (20 μg) were mixed with equal volumes of loading buffer (0.5 M Tris-HCl pH 6.8, 20% glycerol, 10% SDS, 1.5% bromophenol blue, 5% β-mercaptoethanol). Samples were dipped in boiling water for 5 minutes then loaded on 8% SDS-PAGE gel. Electrophoresis was conducted in running buffer (25 mM Tris base, 192 mM glycine, 0.1% SDS). For the first 30 minutes, the run was conducted under 60 V then it was increased to 120 V for 90 minutes. Proteins were then transferred into activated polyvinylidene fluoride membrane in transfer buffer (1 L contains: 200 ml of methanol, 2.4 g of Tris base, 14.2 g of glycine, 0.1 g of SDS) at 140 V for 2 hours. Thereafter, the membrane was incubated overnight at 4°C with blocking buffer containing 5% skimmed milk and 0.5% bovine serum albumin (BSA) in Tris-buffered saline containing 0.1% (vol/vol) Tween-20 (TBS-T). Then, membranes were thoroughly washed in TBS-T and then probed with antiphosphotyrosine (Y^{705}) STAT3 monoclonal antibody at a 1:500 dilution for 2 hours. The membrane was then washed five times (5 minutes per wash) with TBS-T under gentle shaking. Then, goat antimouse polyclonal Ab at 1:50,000 was added to the membranes in blocking buffer and kept at room temperature for 90 minutes under gentle shaking. The membrane was then washed five times (5 minutes per wash) with TBS-T under gentle shaking and developed using ECL Plus Detection Kit. The membranes were incubated with stripping solution (100 mM β-mercaptoethanol in TBS-T) at 37°C for 30 minutes. They were then washed, blocked, and probed with anti-STAT3 Ab and antiactin Ab (I-19) at 1:1000 dilution. Membranes were developed using ECL Plus Detection Kit.

MTT assay. B16 cells, grown in 96-well flat-bottomed microplates, were treated as indicated. Thereafter, 100 μl of MTT solution in culture medium (0.5 mg/ml) was added to each well for 2 hours. The formed formazan crystals were dissolved by adding 200 μl of dimethyl sulfoxide to each well. Optical density was measured at 550 nm using a microplate reader (Powerwave with KC Junior software; Bio-Tek, Winooski, VT). The results were converted into percentage viability relative to the untreated sample.

Caspase 3 activity assay. The caspase 3 activity was measured as an indicator for apoptosis. For that purpose, B16 cells were treated with 50 nM siRNA in PEI or PEI-StA for 24 hours. Using caspase 3 assay kit, cells were normalized for 10^5 cells per treatment group, lysed, and placed in designated wells in 96-well flat-bottomed microplates. Provided caspase 3 inhibitor (Ac-DEVD-CHO) and caspase 3 substrate (Ac-DEVD-pNA) were then added to designated wells according to the manufacturer's instructions. Optical density was measured at 405 nm using microplate reader, and caspase 3 activity was calculated based on p-nitroaniline calibration curve.

Flow cytometry analysis. For phenotypic maturation studies, 1×10^5 DC primary cultures were washed with PBS and suspended in FCM buffer (PBS with 5% FBS). Then, cells were incubated with CD86 and CD40 mAbs or corresponding isotype controls and kept in 4°C for 30 minutes. After that, cells were washed three times with FCM buffer to remove excess mAbs, and all samples were finally acquired on a Becton-Dickinson FACS and analyzed by Cell-Quest software (BD Biosciences, Franklin Lakes, NJ).

Mixed lymphocyte reaction. T cells were obtained from spleen of BALB/c mice Jackson Laboratory. Spleen was crushed between two slides, and T cells were purified using EasySep Negative Selection kit according to the manufacturer's instructions. Purified T cells were cocultured in flat-bottomed 96-well plates with irradiated DCs at a ratio of 2:1 in 37°C and 5% CO_2. Thereafter, [^{3}H]-thymidine was added during the last 18 hours of a 3-day coculture, and the T-cell proliferation was measured by [^{3}H]-thymidine incorporation in counts per minute. The corresponding secretion of IL-2 was determined by ELISA in a 96-well microplate using a microplate reader (Powerwave with KC Junior software; Bio-Tek) at an optical density of 450 nm with reference set at 570 nm. All samples were analyzed in at lease triplicates.

Assessing the Effect of Anti-STAT3 siRNA Complex Treatment of B16 Tumors on Immune Response In Vivo

Tumor establishment and treatment. B16 tumor was established as described earlier in Alshamsan et al. [18]. In brief, 0.75×10^6 B16 cells were inoculated subcutaneously in the upper left flank of male C57BL/6 mice. After 10 days, 500 pmol of STAT3-targeting siRNA complexes (PEI and PEI-StA) or NT siRNA complexes (PEI[NT] and PEI-StA[NT]) in normal saline were administered to randomly assigned groups (five to seven mice per group) by intratumoral (i.t.) injections on daily basis for 4 days. siRNA complexes were freshly prepared before each administration as described previously in Alshamsan et al. [18]. Additional control group received daily i.t. injections of normal saline without any formulation.

Assessing tumor growth and STAT3 expression. Tumor dimensions were measured by vernier caliper after 1 day of the final treatment dose. Tumor volume was calculated as follows:

$$\text{Tumor Volume } (\text{mm}^3) = \frac{\text{Longest Diameter} \times \text{Perpendicular Diameter}^2}{2}$$

Thereafter, mice were killed; tumor samples were immediately isolated and crushed between two slides to form uniform cell suspension and analyzed for STAT3 expression by Western blot as described in the *in vitro* study.

Evaluating the immunologic profile in tumor milieu. Supernatants of each tumor sample were analyzed for protein content by Micro BCA Protein Assay, normalized, and analyzed for IL-12, TNF-α, and IFN-γ using corresponding ELISA kit as mentioned earlier. Furthermore, immune cells were evaluated for cell percentage and activation level by FCM as previously mentioned. For that purpose, each cell suspension was incubated with antimouse CD3, CD4, CD8, NK1.1, CD11c, CD86, and CD40 mAbs or corresponding isotype controls and kept in 4°C for 30 minutes. Then, cells were washed three times with FCM buffer to remove excess mAbs, and 1×10^6 cells were finally acquired from each sample on a Becton-Dickinson FACS and analyzed by Cell-Quest software.

Evaluation of DC functionality after siRNA treatment in vivo. To assess DC functionality in tumor-bearing mice after STAT3 knockdown, MLR was conducted. Splenocytes from each treatment group were isolated, irradiated, and cocultured with purified T cells from BALB/c mice in 37°C and 5% CO_2. T-cell proliferation was measured as described earlier. Similarly, IL-2 level in each sample was measured by ELISA as described earlier.

Data Analysis

Data were analyzed for statistical significance ($P < .05$) by one-way analysis of variance; *post hoc* Scheffé test was conducted to determine level of significance (Version 16.0; SPSS for Windows; IBM, Chicago, IL).

Results

STAT3 Knockdown in B16 by siRNA Induces DC Maturation and Activation In Vitro

We have previously shown that, on exposure to B16-CM, DCs remain in the inactive state [21]. The results of this study demonstrated that the immunosuppressive effect of B16-CM on DCs could be reversed by silencing STAT3 in B16 cells before DC exposure. Targeting B16 cells with anti-STAT3 siRNA in PEI and PEI-StA complexes caused knockdown of STAT3 expression in a specific and dose-dependent fashion (Figure 1, *A* and *B*). However, PEI-StA complexes showed superior inhibitory effect on the level of p-STAT3 expression (compared with PEI) as evidenced by the increase in p-STAT3 silencing percentage at most concentrations tested (Figure 1*A*). When B16 cells were treated with an siRNA concentration of 50 nm, complexes formed by PEI-StA have induced a significant knockdown of the level of both p-STAT3 and STAT3 compared with PEI-treated group (Figure 1*B*). This corresponded to a cytotoxic effect on B16 cancer cells as shown by up to 30% reduction in cell viability (Figure 1*C*, *top panel*) and more than twofolds induction in the activity of the apoptotic protein caspase 3 (Figure 1*C*, *bottom panel*). The exposure of DCs to B16-CM from B16 cells in which STAT3 was silenced by PEI or PEI-StA/siRNA complexes induced phenotypic DC maturation indicated by the significantly higher surface expression of CD86 and CD40 compared with controls. For both markers, the surface expression was higher by B16-CM/PEI-StA treatment where it allowed for an induction reaching 89% for CD86 (Figure 2*A*) and 66% for CD40 (Figure 2*B*) higher than that of B16-CM/PEI treatment. Bar graphs show mean fluorescence intensity (MFI) values after each treatment where B16-CM/PEI-StA treatment gives more MFI signals than treatments with controls ($^*P < .05$) and B16-CM/PEI ($^aP < .05$) for both CD86 and CD40. Consistently, DCs activity, characterized by their ability in recognition and priming of allogenic T cells, was also restored after STAT3 silencing in B16 cells (Figure 2*C*). T cells cocultured with DCs from B16-CM/PEI or B16-CM/PEI-StA groups showed a significant increase in their proliferation compared with controls ($P < .05$). Similar to the phenotypic DC maturation results, DCs showed enhanced functionality when exposed to B16-CM/PEI-StA compared with B16-CM/PEI ($P < .05$; Figure 2*C*, *left panel*). It is worth noting that IL-2 that is concomitantly secreted from T cells during their proliferation followed a similar pattern where its maximum level was detected after T-cell coculture with DCs from B16-CM/PEI-StA group (Figure 2*C*, *right panel*). This is consistent with our FCM results because DCs exposed to B16-CM/PEI-StA showed a significantly higher expression of costimulatory molecules compared with that of B16-CM/PEI (data from Figure 2, *A* and *B*).

Tumor Growth Inhibition after STAT3 Knockdown In Vivo

Tumor growth study after STAT3 knockdown in B16 tumors by siRNA revealed significant tumor regression of the treated tumor masses compared with controls as a result of STAT3 knockdown (Figure 3*A*). PEI-StA complexes significantly reduced tumor growth compared with saline-treated control ($P < .05$) and PEI-treated group ($P < .05$). In fact, tumor volume analysis confirmed uniformity of treatment and response as indicated by close adherence of subjects in each group to the group average (Figure 3*A*, *top panel*). Average tumor volume dramatically dropped from ~390 mm^3 in the untreated group to ~170 mm^3 in case of PEI complexes. It is worth noting that further reduction in tumor volume was noticed with PEI-StA complexes where it reached ~42 mm^3 after 24 hours of the final treatment dose. Similarly, STAT3 expression *in vivo*, measured in isolated tumors 1 day after the final treatment dose, was significantly reduced on siRNA administration by PEI and PEI-StA complexes reaching 25% and 55% less than that of saline-treated control, respectively (Figure 3*A*, *bottom panel*). Figure 3*B* shows the representative three

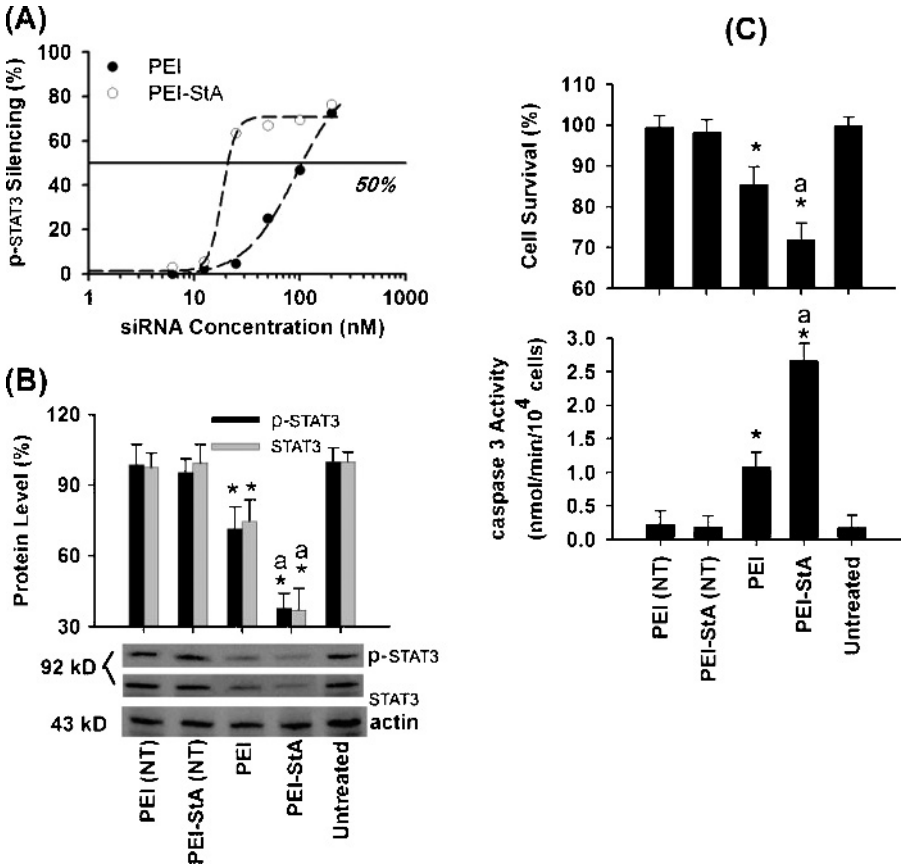

Figure 1. B16.F10 cell death after STAT3 knockdown by anti-STAT3 siRNA complexes *in vitro*. (A) Confluent B16 cells were incubated for 36 hours with titrated doses of anti-STAT3 siRNA (6.25-400 nM) delivered by PEI or PEI-StA complexes. The cells were then lysed, and p-STAT3 levels were detected by Western blot as explained in details in the Materials and Methods section. Percentage of p-STAT3 silencing was calculated at each dose by comparing level of STAT3 of test group *versus* level of STAT3 in the untreated cells (considered as 100%). The dose-response curve of p-STAT3 silencing percentage was plotted against anti-STAT3 siRNA concentration using a four-parameter logistic function. (B) A representative Western blot analysis of B16 cells when treated with 50 nm of anti-STAT3 siRNA delivered by PEI or PEI-StA complexes. Identical complexes of NT siRNA as well as untreated B16 cells were used as controls. Bands' optical intensities of p-STAT3 (black bars) and STAT3 (gray bars) were quantified and normalized to actin bands using the ImageJ software. Data are shown as mean ± SD of four experiments. Statistical significance was determined compared with control (*$P < .05$) and PEI-treated ($^aP < .05$) groups. (C) Cell viability as well as apoptosis after 600 designated treatment were assessed by MTT assay (top) and caspase 3 activity assay (bottom), respectively. Caspase 3 activity after the designated treatment was calculated as the difference in the rates of substrate cleavage in the samples with and without specific caspase 3 inhibitor and expressed as nanomoles per minute per 10^4 cells. Data are shown as mean ± SD of seven to eight replicates for each sample. Statistical significance was determined compared with control (*$P < .05$) and PEI-treated ($^aP < .05$) groups.

mice per treatment group at the end point of the study (after 24 hours of final treatment). Our current results are consistent with our previous findings where the stearic acid derivative of PEI increased both stability and potency of siRNA *in vitro* and *in vivo* [18,19]. The results also indicate a uniformity in response to treatment, where each single subject who received the anti-STAT3 siRNA PEI or PEI-StA complexes showed a reduction in tumor mass compared with NT or untreated controls. Besides, the antitumor effect was better in each single subject of the PEI-StA group compared with PEI group, indicating the potency provided by the lipid-modified formulation.

Induction of DC Activation In Vivo *after STAT3 Knockdown in B16 Tumor*

To evaluate DC infiltration and activation, FCM analysis was performed for the DC lineage marker CD11c and activation markers CD86 and CD40 in tumor cell suspensions after designated treatments of B16 tumors. Our results demonstrate up to an approximately fourfold increase in $CD11c^+$ DC infiltration in B16 tumor mass on STAT3 knockdown (Figure 4*A*, *top panel*). However, no statistically significant difference was noted between PEI and PEI-StA treatment groups. In PEI and PEI-StA groups, further analysis of DC population showed an increase in the surface expression of both CD86 and CD40, reaching up to 35% and 48% higher than NT siRNA and saline control treatments (Figure 4*A*, *bottom panel*). PEI-StA complexes of STAT3 siRNA also allowed for an increase in CD86 and CD40 expression that was 16% higher than that of PEI complexes. Moreover, ELISA analysis of tumor supernatants indicated the production of high levels of proinflammatory cytokines IL-12 and TNF-α after STAT3 knockdown (Figure 4*B*). The results clearly show that PEI-StA complexes allowed for a significant increase in TNF-α and IL-12 production that was 38% and 129% higher than what was measured with PEI complexes, respectively.

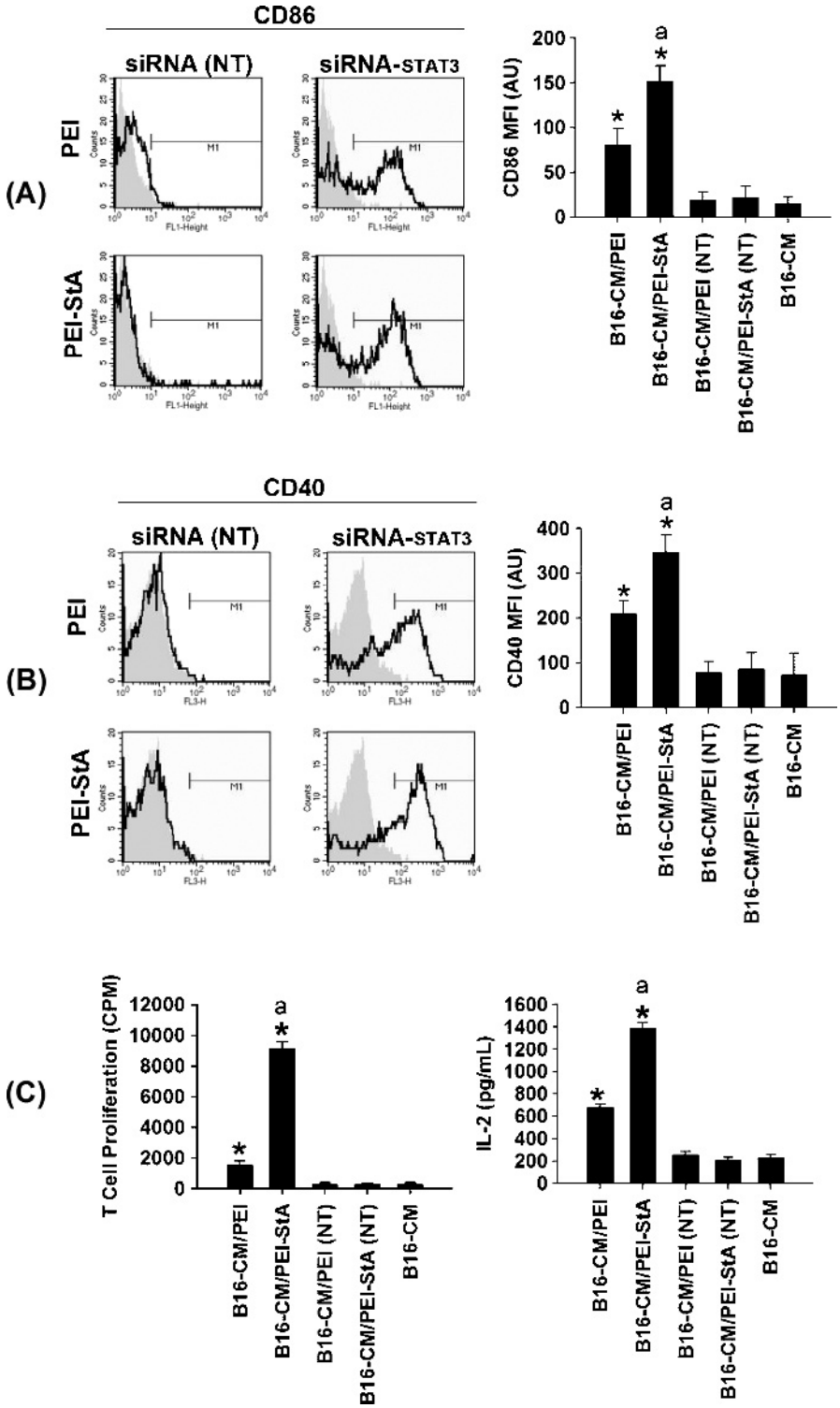

Figure 2. Restoration of DC phenotypic maturation *in vitro*. Primary DC cultures in day 7 were incubated with B16-CM of B16 culture that was treated with anti-STAT3 siRNA or NT siRNA complexes of PEI or PEI-StA for 24 hours. (A, B) FCM analysis of CD86 and CD40 expression on the DC surface, respectively. In histograms (left), black lines indicate DCs exposed to B16-CM from siRNA-treated groups (whether anti-STAT3 or s.c.), whereas gray shade indicates DCs exposed to untreated B16-CM control. Bar graphs (right) shows MFI values after each treatment. Data are presented as a mean of three different measurements (±SD). (C) STAT3 knockdown in DCs restores the capability of DCs to stimulate allogenic T-cell responses. Bars represent the level of T-cell proliferation (left) and IL-2 levels detected in the culture supernatant (right). All data are shown as mean ± SD of at least triplicates for each sample. Statistical significance was determined compared with control (*$P < .05$) and PEI-treated ($^{a}P < .05$) groups.

Alloreactivity of DCs from Tumor-Bearing Mice

To evaluate the functional maturation of DCs after STAT3 knockdown *in vivo*, MLR between irradiated splenocytes from tumor-bearing and allogenic T cells was conducted. As shown in (Figure 4*C*, *top panel*), high allogenic T-cell proliferation was recorded after coculture with splenocytes from the STAT3 knockdown groups treated with PEI and PEI-StA complexes. In addition, the measured cpm was 1.5 times higher in the PEI-StA group than that in the PEI. This was in agreement with our previous FCM results where PEI-StA induced the highest expression of costimulatory molecules on DC surface *in vivo* (data from Figure 4*A*). Consistently, IL-2 production concomitant to T-cell proliferation in PEI-StA group was around double of that for the PEI group (Figure 4*C*, *bottom panel*). These results indicate more distal effects of local intratumoral silencing of STAT3 in B16 tumor by siRNA complexes particularly those of PEI-StA.

Tumor Infiltration of T Cells after STAT3 Knockdown

FCM analysis was conducted in tumor cell suspensions for CD3 expression, the signaling part of the T-cell receptor (TCR) complex. As shown in Figure 5 (*left panel*), STAT3 knockdown in B16 tumor allowed for a profound $CD3^+$ lymphocyte infiltration into tumor mass reaching more than three- and fivefold increases with PEI and PEI-StA groups compared with saline control, respectively. Differential analysis of $CD3^+$ population indicates an increase in $CD4^+$ T helper cells, $CD8^+$ cytotoxic T cells, and NKT cells (Figure 5, *right panel*). Moreover, because activated T cells produce IFN-γ, we measured the level of this cytokine in tumor cell supernatant. The ELISA results detected a significant production of IFN-γ after STAT3 knockdown, where PEI-StA allowed for ~48% higher cytokine level than PEI treatment (Figure 5, *left panel*). This immunostimulatory profile strongly suggests a role of the immune response in the antitumoral effect recorded with siRNA-mediated STAT3 knockdown in B16 cells.

Discussion

Compelling evidence supporting the promise of interrupting STAT3 signaling pathway as a strategy for cancer therapy in solid and hematological tumors (reviewed in Al Zaid Siddiquee and Turkson [22]) has accumulated. Recent studies on melanoma patients suggested that tyrosine-phosphorylated STAT3 is a valid biomarker for atypical nevi progression [23]. Moreover, activated STAT3 was found to have permanent DNA-binding activity in primary human melanoma samples but not normal skin samples from the same patients [24]. Hence, STAT3 was considered a potential target for chemoprevention and treatment of melanoma. Furthermore, numerous studies showed that targeting STAT3 in melanoma tumor models leads to the induction of tumor regression [25], inhibition of angiogenesis [26], prevention of metastasis [27], as well as activation of immune response [3,4]. Because constitutively activated STAT3 in tumors would negatively influence multiple subsets of immune cells, it is logical to expect an induction of the immune response after STAT3 disruption in tumors.

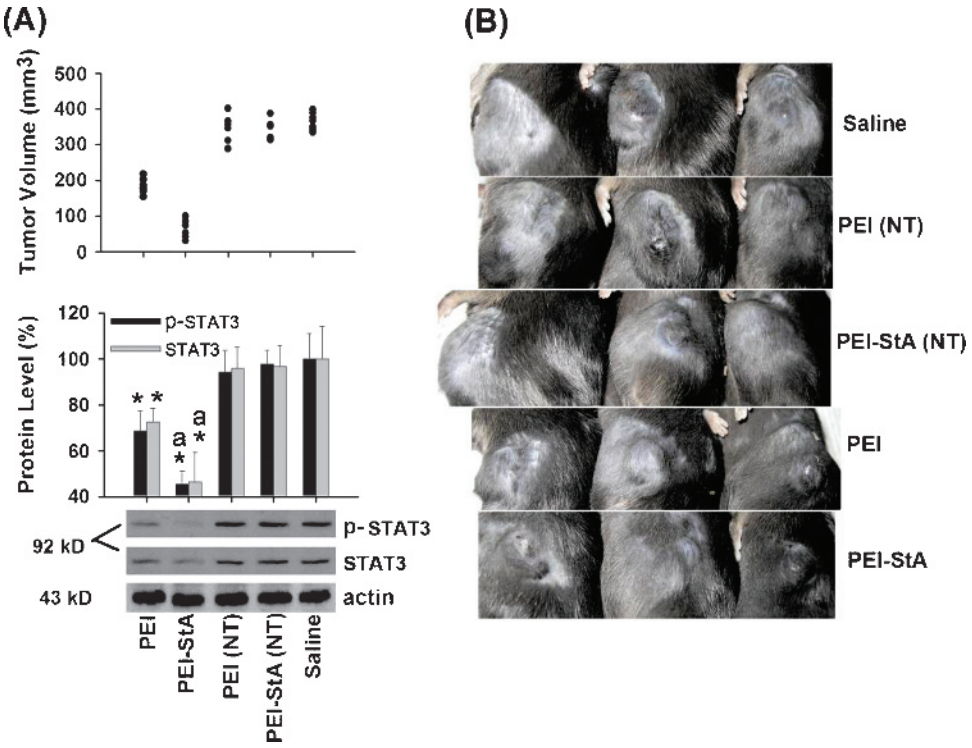

Figure 3. Tumor regression after STAT3 knockdown by anti-STAT3 siRNA complexes. B16 cells were inoculated subcutaneously (0.75×10^6 cells per mice). NT or anti-STAT3 siRNA were administered daily by i.t. route from day 10 to day 13. At day 14, tumor dimensions were obtained, and tumor volume was calculated accordingly for each subject. Isolated tumors from each group were then lysed for Western blot analysis. (A) The value of tumor volume was plotted for each subject and presented as closed circles (top). Western blot analysis (bottom) shows the expression level of p-STAT3, STAT3, and actin loading control. Bands' optical intensities of p-STAT3 (black bars) and STAT3 (gray bars) were quantified and normalized to actin bands using ImageJ software. Data are shown as mean ± SD of four experiments. Statistical significance was determined compared with control ($^*P < .05$) and PEI-treated ($^aP < .05$) groups. (B) Pictures of three representative mice per treatment group at the end point of the study (24 hours after last dose).

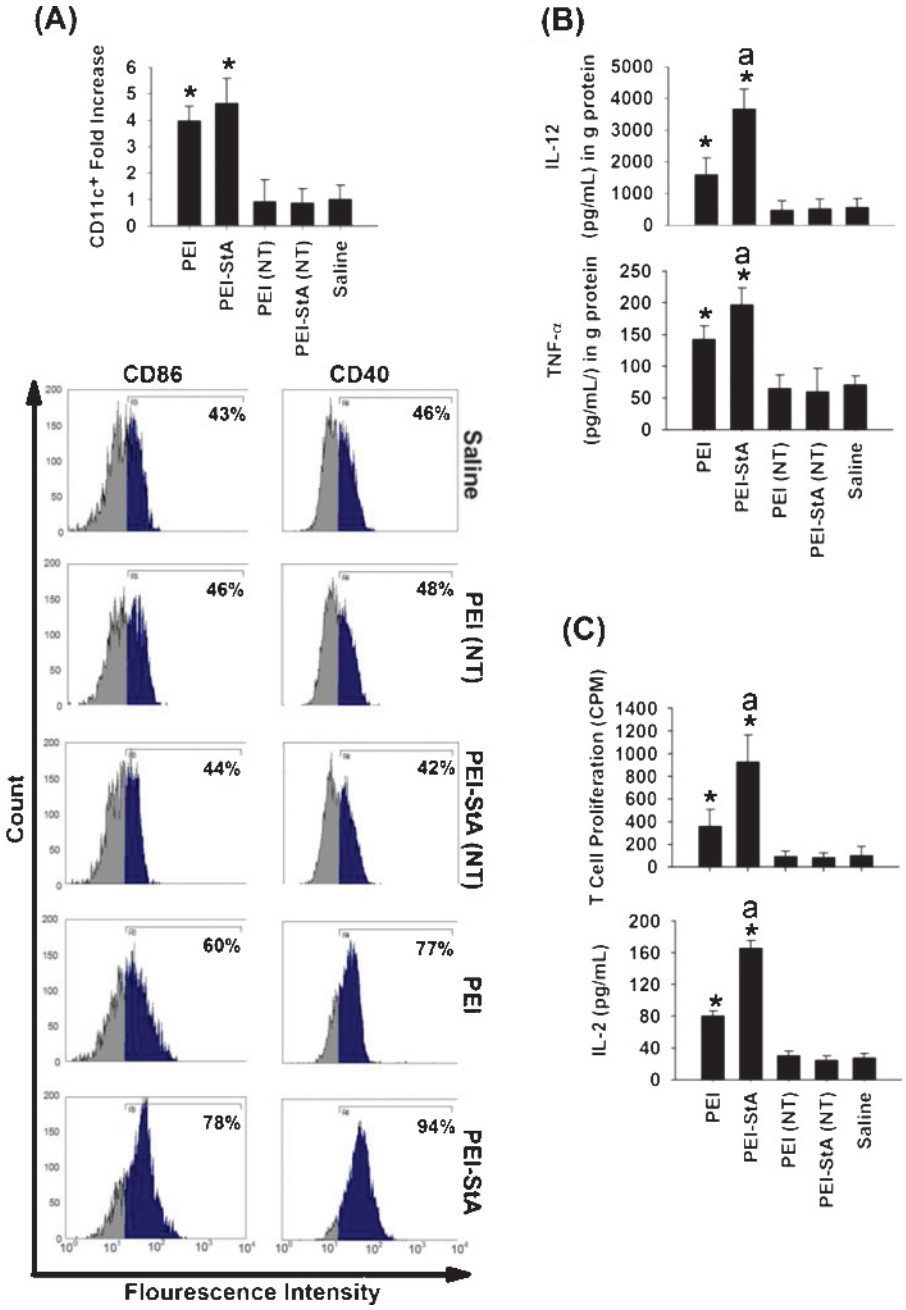

Figure 4. Activation of tumor-infiltrating DCs *in vivo*. At the end point of siRNA treatment (as described in Figure 3), tumor samples were isolated and crushed between two slides into uniform cell suspensions. Cellular component as well as supernatant of each group was analyzed by FCM and ELISA, respectively. (A) Bar graph (top) represents the fold increase of $CD11c^+$ cells in the tumor cell suspensions of different treatment groups (compared with saline-treated group). Data are shown as mean ± SD of three measurements. Statistical significance was determined compared with control (*$P < .05$). Histograms (bottom) show the expression pattern of DC activation markers CD86 and CD40 in the tumor cell suspensions obtained from different treatment groups. The percentage of cells of the gated population is indicated in the upper right corner of each histogram, whereas the populations of cells in-gate and out-of-gate were separated by the vertical line in each histogram. (B) Cytokine levels measured in tumor sample supernatants by ELISA were plotted in bar graphs for IL-12 (top) and TNF-α (bottom). Data are shown as mean ± SD of three measurements. Statistical significance was determined compared with control (*$P < .05$) and PEI-treated ($^a P < .05$) groups. (C) Allogenic MLR after STAT3 silencing *in vivo*. Splenocytes from tumor-bearing mice were collected, irradiated, and cocultured with allogenic T cells. Bars represent the level of T-cell proliferation (top), and IL-2 levels were detected in the supernatant (bottom). All data are shown as mean ± SD of five replicates for each sample. Statistical significance was determined compared with control (*$P < .05$) and PEI ($^a P < .05$).

In fact, such effect is not thought to be totally associated with direct STAT3 disruption in immune cells because they were not intended for manipulation but rather a consequence for the anti-STAT3 effect in tumor cells, that is, a bystander effect.

Bystander effects as a result of STAT3 inhibition were first described in B16 murine melanoma transfected with dominant-negative form of STAT3 [28]. In that study, unpredicted cytotoxicity was noted in neighboring tumor cells that never received the dominant-negative

treatment. Subsequent studies in this focus have isolated three possible mechanisms after STAT3 inhibition by which bystander effects could be mediated: (i) production of soluble factors that induce tumor apoptosis [29], (ii) suppressed angiogenesis as determined by VEGF down-regulation [26], and (iii) involvement of innate and adaptive antitumor immune response as indicated by the production of proinflammatory mediators and infiltration of macrophages, neutrophils, and T cells in the tumor mass [3,10]. The last that gained special focus of the scientific community as a widely progressing area of research today comprises chemotherapy and immunotherapy for cancer [30].

We have recently showed that siRNA-mediated STAT3 silencing in B16.F10 via intratumoral administration of siRNA/PEI complexes results in a remarkable tumor regression [18]. Along with direct tumor apoptosis, molecular investigation in that study revealed two possible bystander effects: increase in IL-6 and decrease in VEGF levels in tumor microenvironment [18]. We hypothesized that the antitumor activity observed subsequent to STAT3 knockdown is partly owed to the breakdown of immunosuppressive microenvironment leading to improvements in DC maturation, immune cell activation, and trafficking to the tumor. The validity of this hypothesis was investigated in the current study through assessing the bystander immune response after STAT3 knockdown in B16 melanoma cells *in vitro* and *in vivo* using siRNA complexes of PEI and its stearic acid derivative. In our approach to evaluate the immunologic picture after siRNA intervention, we focused on three aspects: the level of immune cell maturation and activation, percentage of tumor-infiltrating lymphocytes, and cytokine profiles in tumor milieu.

DCs are professional antigen-presenting cells that form a crucial link between innate and adaptive immune system. In normal situations, DCs recognize antigens from normal, microbial, or tumoral origins [31]. These antigens get processed and presented in the context of major histocompatibility complex class I and II to be recognized by $CD8^+$ and $CD4^+$ T cells, respectively [32]. Nevertheless, DCs must provide three signals to activate naive T cells: antigen presentation in the context of major histocompatibility complex class I and II (signal 1), costimulation provided by molecules such as CD86 and CD40 that interact with their ligands on T-cell surface (signal 2), and cytokine stimulation (signal 3) to polarize T cells toward intended response, for example, antitumoral response. However, tumors secrete factors that inhibit DC differentiation and maturation and eventually

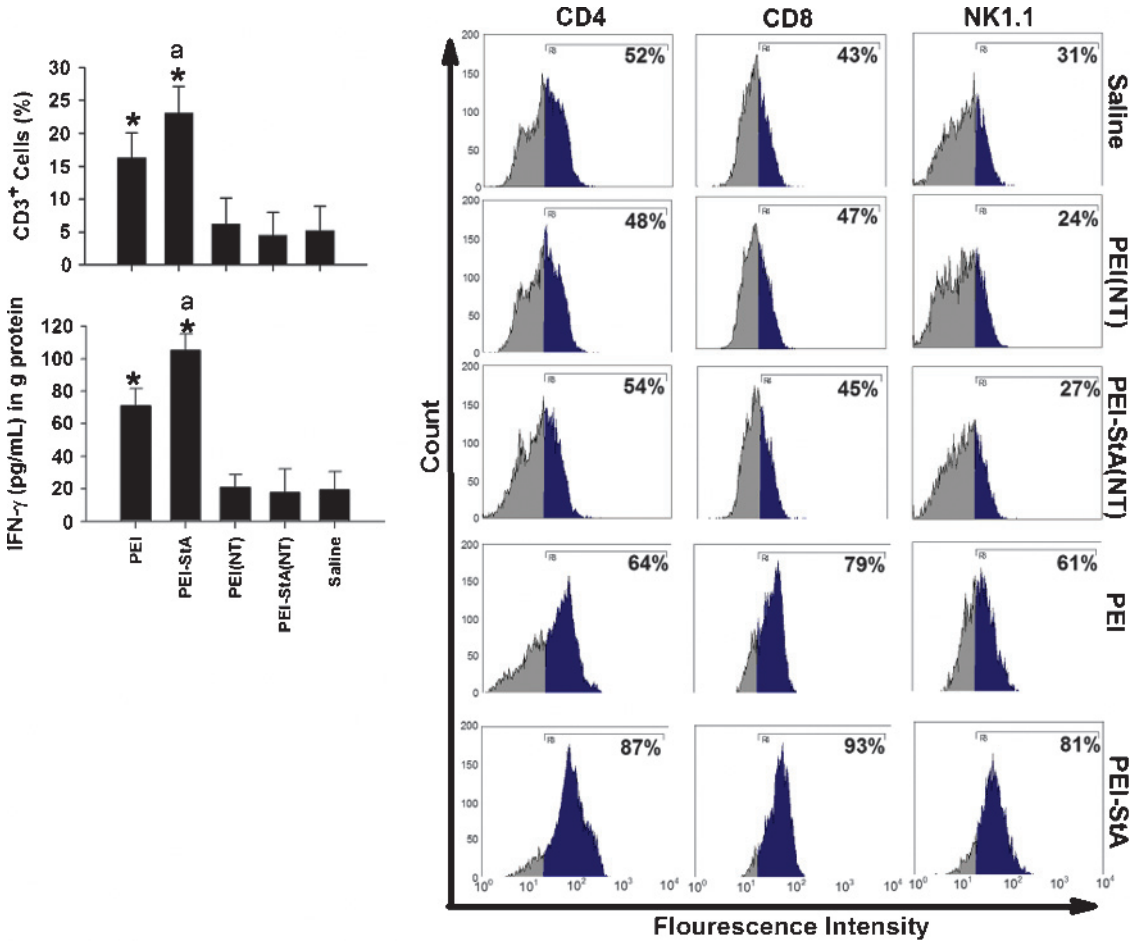

Figure 5. Activation of tumor-infiltrating lymphocytes *in vivo*. Tumor samples from different treatment groups were isolated (as described in Figure 4) and analyzed for the presence and activation of tumor-infiltrating lymphocytes. Bar graphs (left) represent percentages of cells positive for CD3 (T-cell marker) (top) and the amount of IFN-γ detected in the tumor supernatants from different treatment groups (bottom). Data are shown as mean ± SD of three measurements. Statistical significance was determined compared with control (*$P < .05$) and PEI ($^aP < .05$). Histograms (right) show the differential lymphocyte population markers CD4, CD8, and NK1.1 for the designated treatment groups. Percentage of cells of the gated population is indicated in the upper right corner of each histogram, whereas the populations of cells in-gate and out-of-gate were separated by the vertical line in each histogram.

evade the adaptive immune response through this strategy [4]. In fact, DC malfunction due to TDFs is documented in melanoma patients [4]. To mimic this situation, we conducted an *in vitro* study where DCs were exposed to B16-CM with or without siRNA treatment (Figures 1 and 2). Our *in vitro* study indicates that (i) phenotypical and functional maturation of DCs can be restored after cancer cell manipulation with STAT3 siRNA complexes and that (ii) the level of DC activation is correlated with the level of STAT3 knockdown in B16 cells. We show that DC alloreactivity (Figure 2*C*) was noticed only with groups that showed a higher expression of the costimulatory molecules CD86 and CD40 (Figure 2*A* and *B*). This is an important observation because it proves that B16-CM–treated DCs became functional after siRNA manipulation of B16 cells. The CD86 and CD40 molecules on DC surface interact with CD28 and CD40 ligand (CD40L) on T-cell surface. Such interaction is beneficial for both DCs and T cells where stimulation of CD28 stabilizes CD40L on T cells and stimulation of CD40 on DCs increases their expression of CD86 molecules [33,34]. Therefore, functional and phenotypic maturation of DCs are both required for naive T-cell activation. Moreover, we noticed that STAT3 knockdown of B16 cells with PEI-StA complexes of siRNA leads to higher phenotypic and functional maturation of DCs. This is consistent with our previous results where PEI-StA complexes were more potent in STAT3 knockdown and caused higher cell killing effect on B16 cells [18]. One reason for the superior effect of PEI-StA complexes reflected on DC 415 activation is the exponential nature of B16 cell death. It has been suggested that B16 apoptosis after STAT3 disruption involves the production of soluble factors such as TNF-related apoptosis-inducing ligand, which induces tumor cell death [29,35]. Such effect has shown to improve antitumoral function of DCs *in vitro* and *in vivo* [36]. Nevertheless, detailed analysis of B16-CM is still needed to pinpoint factors responsible for DC activation. These proof-of-concept results demonstrate that manipulation of STAT3 in tumor cell culture has a positive effect on DC activation.

A similar effect was noticed after STAT3 knockdown *in vivo*. The recorded B16 tumor regression (Figure 3) was associated with DC activation (Figure 4) and lymphocytes infiltration (Figure 5). Consistent with our previous findings, STAT3 silencing by siRNA/PEI-StA complexes was superior to that of PEI owing to the higher protective effect of PEI-StA toward siRNA [18]. Consequently, we observed a significant infiltration of $CD11c^+$ DCs in tumor tissue (Figure 4*A*, *top panel*). However, we also noted a comparable DC infiltration for groups treated with PEI and PEI-StA complexes. Such picture is quite logical *in vivo* because DCs traffic out of the site of antigen encounter to the spleen and draining lymph node to present the antigen to naive T cells [37]. Considering the fact that DC influx and efflux in and out of tumor mass is a continuous process, whereas the FCM analysis was performed in a specific time point, the difference in DC infiltration between the two formulations is irrelevant. In this case, a more important factor is the level of DC activation. Here we noticed an advantage for PEI-StA over PEI in CD86 and CD40 expression (Figure 4*A*, *bottom panel*) as well as levels of proinflammatory cytokines IL-12 and TNF-α (Figure 4*B*). DCs are known to produce IL-12 and TNF-α on capturing tumor antigen [38]. The production of IL-12 was recently found to be an absolute requirement for T_H1-type immune response that leads to CTL antitumor response [39]. TNF-α was also shown to enhance DC maturation and promote antitumor immune response [40]. The DC activation results were corroborated with our MLR study. Here we show that on STAT3 knockdown *in vivo*, DCs in the spleens of tumor-bearing mice showed more alloreactivity with allogenic T cells (Figure 4*C*). The noted advantage of PEI-StA group supports our argument that activated DCs are home to secondary lymphoid organs because more indicative results are demonstrated in those organs. Moreover, we find the results of clinical significance because some evidence showed that peripheral blood DCs induce lower allogenic MLR in a study done on 32 breast cancer patients [41]. Hence, a high MLR outcome can be considered a positive indicator of the therapeutic approach.

Furthermore, a high level of TIL was recorded after tumor regression after STAT3 knockdown was proved by the high level of $CD3^+$ cells (Figure 5, *left panel*). In that population, the superiority of PEI-StA treatment was noted by the induced infiltration of $CD4^+$ T cells, $CD8^+$ T cells, and NKT cells (Figure 5, *right panel*). This high presence of TIL indicates three incidents in this study: stimulation of an innate immune response after tumor regression, imminent DC activation after siRNA intervention because T-cell immune response is a latent response, and, finally, the noted tumor regression is also mediated by CTL response. The latter is explained by the approximately fourfold reduction in tumor volume after PEI-StA administration compared with PEI. Moreover, IFN-γ was positively correlated with TIL level (Figure 5, *left panel*). This proinflammatory cytokines is produced by activated $CD4^+$ T cells, $CD8^+$ CTL, NK cells, and NKT cells and plays a crucial role in antitumor immunity [42]. In fact, IFN-γ production is directly related to suppression of B16 cell growth [43]. Moreover, the results of *in vivo* DC activation (data from Figure 4) highly correlate with these results because the production of IL-12 by DCs and other phagocytes is known to induce IFN-γ production [39]. TNF-α was demonstrated to induce T-cell activation as well [40]. However, it is also important to know that our siRNA complexes may not have an exclusive effect on cancer cells. *In vivo*, the siRNA complexes might have directly affected immune cells as well as cancer cells. This is a therapeutically relevant approach because blocking STAT3 in tumor as well as immune cells can produce a synergistic antitumor effect [10]. Such effect was evidenced by the elegant work of Hua Yu's group where the authors demonstrated the requirement of immune cells for tumor regression using tumor-bearing mouse model with $STAT3^{-/-}$ hematopoietic system [6]. Taken together, the collective picture of our work proves that manipulation of tumoral STAT3 is crucial for the generation of robust innate and adaptive immune responses.

Conclusions

We developed polymeric nontoxic formulations of siRNA for specific STAT3 knockdown in B16 tumor. The siRNA-mediated silencing of STAT3 in B16 melanoma cells was found to be able to break the state of immune tolerance used by the tumor and induce bystander antitumor innate and adaptive immune response. We also found that the bystander effect is highly correlated to the siRNA silencing effect and the tumor-killing action. Such strategy. This strategy could be beneficial as an adjuvant therapy along with chemotherapy and/or immunotherapy for cancer.

Acknowledgments

The authors thank the Research Center, College of Pharmacy, Deanship of Scientific Research, King Saud University, Riyadh, Saudi Arabia.

References

[1] Hanahan D and Weinberg RA (2000). The hallmarks of cancer. *Cell* **100**(1), 57–70.

[2] Pardoll D (2003). Does the immune system see tumors as foreign or self? *Annu Rev Immunol* **21**, 807–839.

[3] Wang T, Niu G, Kortylewski M, Burdelya L, Shain K, Zhang S, Bhattacharya R, Gabrilovich D, Heller R, Coppola D, et al. (2004). Regulation of the innate and adaptive immune responses by STAT-3 signaling in tumor cells. *Nat Med* **10**(1), 48–54.

[4] Kortylewski M, Jove R, and Yu H (2005). Targeting STAT3 affects melanoma on multiple fronts. *Cancer Metastasis Rev* **24**(2), 315–327.

[5] Cheng F, Wang HW, Cuenca A, Huang M, Ghansah T, Brayer J, Kerr WG, Takeda K, Akira S, Schoenberger SP, et al. (2003). A critical role for STAT3 signaling in immune tolerance. *Immunity* **19**(3), 425–436.

[6] Kortylewski M, Kujawski M, Wang T, Wei S, Zhang S, Pilon-Thomas S, Niu G, Kay H, Mule J, Kerr WG, et al. (2005). Inhibiting STAT3 signaling in the hematopoietic system elicits multicomponent antitumor immunity. *Nat Med* **11**(12), 1314–1321.

[7] Buettner R, Mora LB, and Jove R (2002). Activated STAT signaling in human tumors provides novel molecular targets for therapeutic intervention. *Clin Cancer Res* **8**, 945–954.

[8] Hirano T, Ishihara K, and Hibi M (2000). Roles of STAT3 in mediating the cell growth, differentiation and survival signals relayed through the IL-6 family of cytokine receptors. *Oncogene* **19**(21), 2548–2556.

[9] Ivanov VN, Bhoumik A, Krasilnikov M, Raz R, Owen-Schaub LB, Levy D, Horvath CM, and Ronai Z (2001). Cooperation between STAT3 and c-*jun* suppresses Fas transcription. *Mol Cell* **7**(3), 517–528.

[10] Kortylewski M and Yu H (2007). STAT3 as a potential target for cancer immunotherapy. *J Immunother* **30**(2), 131–139.

[11] Kortylewski M and Yu H (2008). Role of STAT3 in suppressing anti-tumor immunity. *Curr Opin Immunol* **20**(2), 228–233.

[12] Yu H, Kortylewski M, and Pardoll D (2007). Crosstalk between cancer and immune cells: role of STAT3 in the tumour microenvironment. *Nat Rev Immunol* **7**(1), 41–51.

[13] Xu Q, Briggs J, Park S, Niu G, Kortylewski M, Zhang S, Gritsko T, Turkson J, Kay H, Semenza GL, et al. (2005). Targeting STAT3 blocks both HIF-1 and VEGF expression induced by multiple oncogenic growth signaling pathways. *Oncogene* **24**(36), 5552–5560.

[14] Nefedova Y, Nagaraj S, Rosenbauer A, Muro-Cacho C, Sebti SM, and Gabrilovich DI (2005). Regulation of dendritic cell differentiation and antitumor immune response in cancer by pharmacologic-selective inhibition of the Janus-activated kinase 2/signal transducers and activators of transcription 3 pathway. *Cancer Res* **65**(20), 9525–9535.

[15] Cejka D, Losert D, and Wacheck V (2006). Short interfering RNA (siRNA): tool or therapeutic? *Clin Sci (Lond)* **110**(1), 47–58.

[16] Hede K (2005). Blocking cancer with RNA interference moves toward the clinic. *J Natl Cancer Inst* **97**(9), 626–628.

[17] Thomas M, Lu JJ, Chen J, and Klibanov AM (2007). Non-viral siRNA delivery to the lung. *Adv Drug Deliv Rev* **59**(2-3), 124–133.

[18] Alshamsan A, Hamdy S, Samuel J, El-Kadi AO, Lavasanifar A, and Uludag H (2010). The induction of tumor apoptosis in B16 melanoma following STAT3 siRNA delivery with a lipid-substituted polyethylenimine. *Biomaterials* **31**(6), 1420–1428.

[19] Alshamsan A, Haddadi A, Incani V, Samuel J, Lavasanifar A, and Uludag H (2009). Formulation and delivery of siRNA by oleic acid and stearic acid modified polyethylenimine. *Mol Pharm* **6**(1), 121–133.

[20] Lutz MB, Kukutsch N, Ogilvie AL, Rossner S, Koch F, Romani N, and Schuler G (1999). An advanced culture method for generating large quantities of highly pure dendritic cells from mouse bone marrow. *J Immunol Methods* **223**(1), 77–92.

[21] Alshamsan A, Hamdy S, Das S, Lavasanifar A, Samuel J, and El-Kadi AO (2010). Bone marrow derived dendritic cells are more suitable than dendritic cell line DC2.4 to study tumor-mediated suppression of DC maturation through STAT3 hyperactivation. *J Pharm Pharmaceut Sci* **13**(1), 21–26.

[22] Al Zaid Siddiquee K and Turkson J (2008). STAT3 as a target for inducing apoptosis in solid and hematological tumors. *Cell Res* **18**(2), 254–267.

[23] Wang W, Edington HD, Rao UN, Jukic DM, Wang H, Shipe-Spotloe JM, and Kirkwood JM (2008). STAT3 as a biomarker of progression in atypical nevi of patients with melanoma: dose-response effects of systemic IFNα therapy. *J Invest Dermatol* **128**(8), 1997–2002.

[24] Niu G, Bowman T, Huang M, Shivers S, Reintgen D, Daud A, Chang A, Kraker A, Jove R, and Yu H (2002). Roles of activated Src and STAT3 signaling in melanoma tumor cell growth. *Oncogene* **21**(46), 7001–7010.

[25] Niu G, Heller R, Catlett-Falcone R, Coppola D, Jaroszeski M, Dalton W, Jove R, and Yu H (1999). Gene therapy with dominant-negative STAT3 suppresses growth of the murine melanoma B16 tumor *in vivo*. *Cancer Res* **59**(20), 5059–5063.

[26] Niu G, Wright KL, Huang M, Song L, Haura E, Turkson J, Zhang S, Wang T, Sinibaldi D, Coppola D, et al. (2002). Constitutive STAT3 activity up-regulates VEGF expression and tumor angiogenesis. *Oncogene* **21**(13), 2000–2008.

[27] Xie TX, Wei D, Liu M, Gao AC, Ali-Osman F, Sawaya R, and Huang S (2004). STAT3 activation regulates the expression of matrix metalloproteinase-2 and tumor invasion and metastasis. *Oncogene* **23**(20), 3550–3560.

[28] Catlett-Falcone R, Landowski TH, Oshiro MM, Turkson J, Levitzki A, Savino R, Ciliberto G, Moscinski L, Fernández-Luna JLF, Nuñez G, et al. (1999). Constitutive activation of STAT3 signaling confers resistance to apoptosis in human U266 myeloma cells. *Immunity* **10**, 105–115.

[29] Niu G, Shain KH, Huang M, Ravi R, Bedi A, Dalton WS, Jove R, and Yu H (2001). Overexpression of a dominant-negative signal transducer and activator of transcription 3 variant in tumor cells leads to production of soluble factors that induce apoptosis and cell cycle arrest. *Cancer Res* **61**(8), 3276–3280.

[30] Rass K and Hassel JC (2009). Chemotherapeutics, chemoresistance and the management of melanoma. *G Ital Dermatol Venereol* **144**(1), 61–78.

[31] Segura E and Villadangos JA (2009). Antigen presentation by dendritic cells *in vivo*. *Curr Opin Immunol* **21**(1), 105–110.

[32] Trombetta ES and Mellman I (2005). Cell biology of antigen processing *in vitro* and *in vivo*. *Annu Rev Immunol* **23**, 975–1028.

[33] Yang Y and Wilson JM (1996). CD40 ligand-dependent T cell activation: requirement of B7-CD28 signaling through CD40. *Science* **273**(5283), 1862–1864.

[34] Johnson-Leger C, Christensen J, and Klaus GG (1998). CD28 co-stimulation stabilizes the expression of the CD40 ligand on T cells. *Int Immunol* **10**(8), 1083–1091.

[35] Sheridan JP, Marsters SA, Pitti RM, Gurney A, Skubatch M, Baldwin D, Ramakrishnan L, Gray CL, Baker K, Wood WI, et al. (1997). Control of TRAIL-induced apoptosis by a family of signaling and decoy receptors. *Science* **277**(5327), 818–821.

[36] Schumacher LY, Vo DD, Garban HJ, Comin-Anduix B, Owens SK, Dissette VB, Glaspy JA, McBride WH, Bonavida B, Economou JS, et al. (2006). Immunosensitization of tumor cells to dendritic cell–activated immune responses with the proteasome inhibitor bortezomib (PS-341, Velcade). *J Immunol* **176**(8), 4757–4765.

[37] Martin-Fontecha A, Lanzavecchia A, and Sallusto F (2009). Dendritic cell migration to peripheral lymph nodes. *Handb Exp Pharmacol* **188**(I), 31–49.

[38] Onishi H, Kuroki H, Matsumoto K, Baba E, Sasaki N, Kuga H, Tanaka M, Katano M, and Morisaki T (2004). Monocyte-derived dendritic cells that capture dead tumor cells secrete IL-12 and TNF-α through IL-12/TNF-α/NF-κB autocrine loop. *Cancer Immunol Immunother* **53**(12), 1093–1100.

[39] Trinchieri G (2003). Interleukin-12 and the regulation of innate resistance and adaptive immunity. *Nat Rev Immunol* **3**(2), 133–146.

[40] Brunner C, Seiderer J, Schlamp A, Bidlingmaier M, Eigler A, Haimerl W, Lehr HA, Krieg AM, Hartmann G, and Endres S (2000). Enhanced dendritic cell maturation by TNF-α or cytidine-phosphate-guanosine DNA drives T cell activation *in vitro* and therapeutic anti-tumor immune responses *in vivo*. *J Immunol* **165**(11), 6278–6286.

[41] Gabrilovich DI, Corak J, Ciernik IF, Kavanaugh D, and Carbone DP (1997). Decreased antigen presentation by dendritic cells in patients with breast cancer. *Clin Cancer Res* **3**(3), 483–490.

[42] Schoenborn JR and Wilson CB (2007). Regulation of interferon-gamma during innate and adaptive immune responses. *Adv Immunol* **96**, 41–101.

[43] Kakuta S, Tagawa Y, Shibata S, Nanno M, and Iwakura Y (2002). Inhibition of B16 melanoma experimental metastasis by interferon-γ through direct inhibition of cell proliferation and activation of antitumour host mechanisms. *Immunology* **105**(1), 92–100.